# Branching Ratios of the $K(1420)$ Meson*

M. Aguilar-Benitez, D. Bassano, R. L. Eisner, J. B. Kinson, and N. P. Samios
*Brookhaven National Laboratory, Upton, New York 11973*

and

V. E. Barnes
*Brookhaven National Laboratory, Upton, New York 11973, and Purdue University, Lafayette, Indiana 47907*
(Received 28 July 1970)

We present a new measurement of the decay rates of the $K(1420)$ produced in $K^-p$ interactions. In addition to improved statistics, the $K(1420)$ is observed in final states where the absence of the $Q$ enhancement allows an unambiguous determination of the branching ratios. The values obtained agree with SU(3) predictions.

Recent controversies about the $A_2(1300)$ meson[1] have caused renewed interest in the properties of other members of the $2^+$ nonet. In this Letter we present a measurement of the decay rates of the $K(1420)$ produced in $K^-p$ interactions. Previous determinations[2] of the number of resonant events in the $K\pi\pi$ final state have suffered either from small statistics or from confusion due to the presence of the $Q$ enhancement in the non-charge-exchange channels. Besides their greater statistical validity, our data encompass the $K^0(1420)n$ final states in which there are clear $K^0(1420)$ signals above background.

The data for this study come from an exposure of the Brookhaven National Laboratory (BNL) 80-in. hydrogen bubble chamber to beams of $K^-$ mesons of 3.9, 4.6, and 5.0 GeV/$c$ incident momenta. The final states of interest are[3] (1) $\bar{K}^0\pi^-\pi^+n$, (2) $K^-\pi^+n$, (3) $\bar{K}^0\pi^-p$, (4) $K^-\pi^-\pi^+p$, (5) $\bar{K}^0\pi^-\pi^0p$, and (6) $K^-\pi^-\pi^+\pi^0p$. Events were assigned to the four-constraint categories if the $\chi^2$ probability was greater than 1% and ionization, as measured by the BNL flying-spot digitizer, was consistent with the kinematic interpretation. For the one-constraint fits, a 5% probability cut was imposed.

The $K(890)\pi$ and $K\rho$ decay rates of the $K(1420)$ were obtained by investigation of Reaction (1) for the combined samples at the three momenta. In Fig. 1(a) the $\bar{K}^0\pi^-\pi^+$ effective-mass spectrum is shown after a peripheral selection, $\cos\theta^*>0.8$, has been imposed ($\theta^*$ is the scattering angle between the target proton and the outgoing neutron in the overall center-of-mass system). A large $K(1420)$ signal is seen with no evidence for a broad low-mass enhancement. The number of $K(1420)$ resonance events was obtained by fitting the mass spectrum with a matrix element containing a Breit-Wigner shape for the $K(1420)$ and a polynomial in the mass variable for the background.[4] The results of the fit are shown as the curve in Fig. 1(a). Figure 1(b) shows the Dalitz plot of $M^2(\bar{K}^0\pi^-)$ vs $M^2(\pi^-\pi^+)$ for the $K(1420)$ region defined as $1.34\leq M(\bar{K}^0\pi^-\pi^+)\leq 1.50$ GeV. A feature of this plot is the large accumulation of events in the $K(890)$-$\rho$ overlap region which is a result of the $\sin^2\theta$ helicity angular distribution of the vector mesons decaying from a parent $2^+$ meson. This makes the branching ratio obtained by selecting $K\pi\pi$ and $\pi\pi$ slices in the $K(890)$ and $\rho$ regions, and using a background subtraction technique, subject to systematic uncertainties. In order to avoid this difficulty, we have directly fitted the Dalitz plot for the $K(1420)$ region by a maximum-likelihood method with the following probability density[5]:

$$|M|^2=\epsilon|M_{1420}|^2+(1-\epsilon)|M_{\mathrm{bkg}}|^2,$$

where $\epsilon=0.37$ is the fraction of resonance events in the $K(1420)$ region determined by the fit[6] to Fig. 1(a) and

$$|M_{1420}|^2=\alpha_1\frac{|f_{\mathrm{BW}}(890)|^2\sin^2\theta_{890}}{\sum\int|f_{\mathrm{BW}}(890)|^2\sin^2\theta_{890}\,d\varphi}+\alpha_2\frac{|f_{\mathrm{BW}}(\rho)|^2\sin^2\theta_\rho}{\sum\int|f_{\mathrm{BW}}(\rho)|^2\sin^2\theta_\rho\,d\varphi},$$

$$|M_{\mathrm{bkg}}|^2=\beta_1\frac{|f_{\mathrm{BW}}(890)|^2}{\sum\int|f_{\mathrm{BW}}(890)|^2\,d\varphi}+\beta_2\frac{|f_{\mathrm{BW}}(\rho)|^2}{\sum\int|f_{\mathrm{BW}}(\rho)|^2\,d\varphi}+\frac{(1-\beta_1-\beta_2)}{\sum\int d\varphi};$$

here $f_{\mathrm{BW}}(x)$ denotes a Breit-Wigner distribution for particle $x$, $\sum\int d\varphi$ signifies integration over the $\bar{K}^0\pi^-\pi^+$ Dalitz plot plus summation over events, $\alpha_1$ ($\alpha_2$) is the $K(1420)$ branching fraction into $K(890)\pi$ ($K\rho$) with[7] $\alpha_1+\alpha_2=1$, and $\sin^2\theta_{890}$ ($\sin^2\theta_\rho$) is the helicity angular distribution of the $\bar{K}^0$ ($\pi^+$) in the rest frame of the $\bar{K}^0\pi^-$ ($\pi^-\pi^+$). The symbol $\beta_1$ ($\beta_2$) represents the fraction of $K(890)$ ($\rho$) in the background

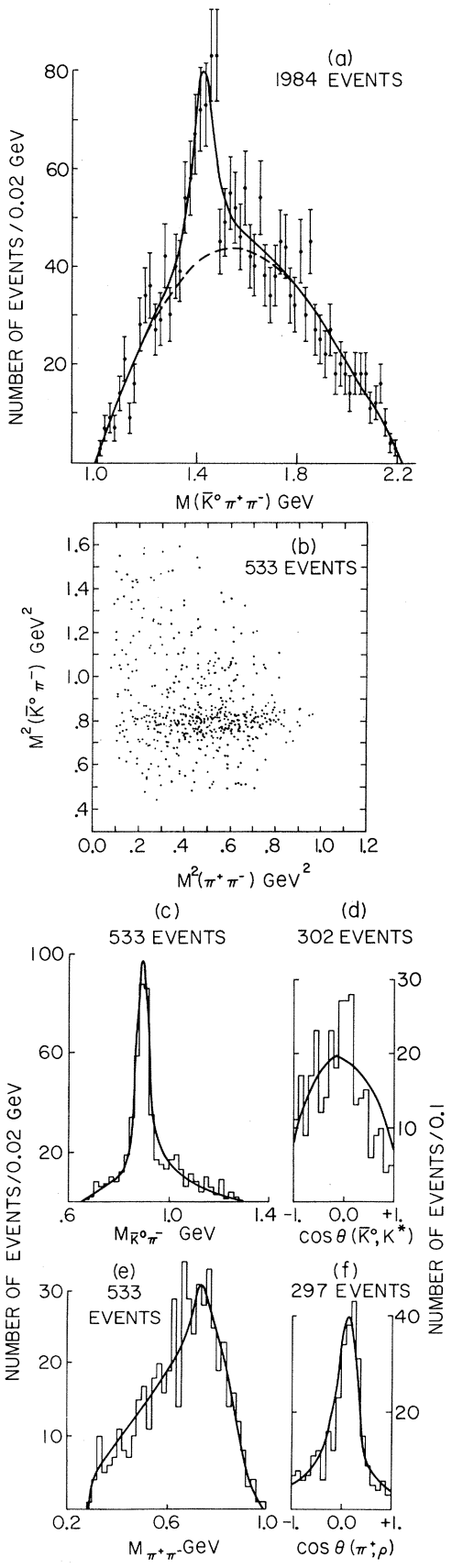


under the $K(1420)$.[8] The results of the maximum-likelihood fit give

$$\alpha_1[K^0(1420) \to K^-(890)(\to \bar{K}^0\pi^-)\pi^+] = 0.80 \pm 0.08,$$

$$\alpha_2[K^0(1420) \to \bar{K}^0\rho^0] = 0.20 \pm 0.08.$$

Figure 1(c) [1(d)] shows the $\bar{K}^0\pi^-$ ($\pi^-\pi^+$) effective-mass projection of the $K(1420)$ Dalitz plot. The helicity angular distributions in the $K(890)$ [$0.84 \leq M(\bar{K}^0\pi^-) \leq 0.94$ GeV] and $\rho$ [$0.63 \leq M(\pi^-\pi^+) \leq 0.89$ GeV] bands are shown in Figs. 1(e) and 1(f). The accompanying curves are the Monte Carlo–generated predictions obtained by using the simple noninterference model and the values of the parameters $\alpha_1$ and $\alpha_2$ given above. The experimental distributions are seen to be well described by the theoretical model.[9]

The $K\pi\pi/K\pi$ branching fractions were obtained by comparison of Reactions (1) and (2) at 3.9 and 4.6 GeV/$c$, separately. Figure 2(a) [2(b)] shows the $K^-\pi^+$ effective-mass spectrum at 3.9 (4.6) GeV/$c$ after a $\cos\theta^* > 0.8$ selection. Figure 2(c) [2(d)] contains the corresponding $\bar{K}^0\pi^-\pi^+$ effective-mass distribution. The number of $K(1420)$ resonant events is derived in a manner similar to that described above, i.e., by fitting the observed mass distribution with a combination of a polynomial in the mass for the background and a noninterfering Breit-Wigner resonance. In Table I we display the number of resonant events and the corresponding cross sections obtained by fitting all these distributions. These involve correcting for undetected decay modes, probability cuts, $V^0$ detection efficiencies, and for the fact that different portions of the film were analyzed for the different final states. Using these cross sections and taking into account Clebsch-Gordan coefficients, the $K(890)\pi/K\pi$ and $K\rho/K\pi$ branching ratios were obtained and are given in Table I.[10] We note that the $K(890)\pi/K\pi$ branching ratio is $0.44 \pm 0.09$ compared with the compiled average[2] of $0.722 \pm 0.087$. All previous experiments

FIG. 1. (a) $\bar{K}^0\pi^-\pi^+$ effective mass spectrum from Reaction (1) for events with $\cos\theta^* > 0.8$. The data at 3.9, 4.6, and 5.0 GeV/$c$ have been combined. There are $273 \pm 38$ $K(1420)$ events as determined from the fit in the manner indicated in the text. (b) $M^2(\bar{K}^0\pi^-)$ vs $M^2(\pi^+\pi^-)$ distribution for events in the $K^0(1420)$ region. (c) $M(\bar{K}^0\pi^-)$ projection of the $K(1420)$ Dalitz plot. (d) Helicity angular distribution in the $K(890)$ rest frame for events in the $K(1420)$ region. (e) $M(\pi^-\pi^+)$ projection of the $K(1420)$ Dalitz plot. (f) Helicity angular distribution in the $\rho$ rest frame for events in the $K(1420)$ region.

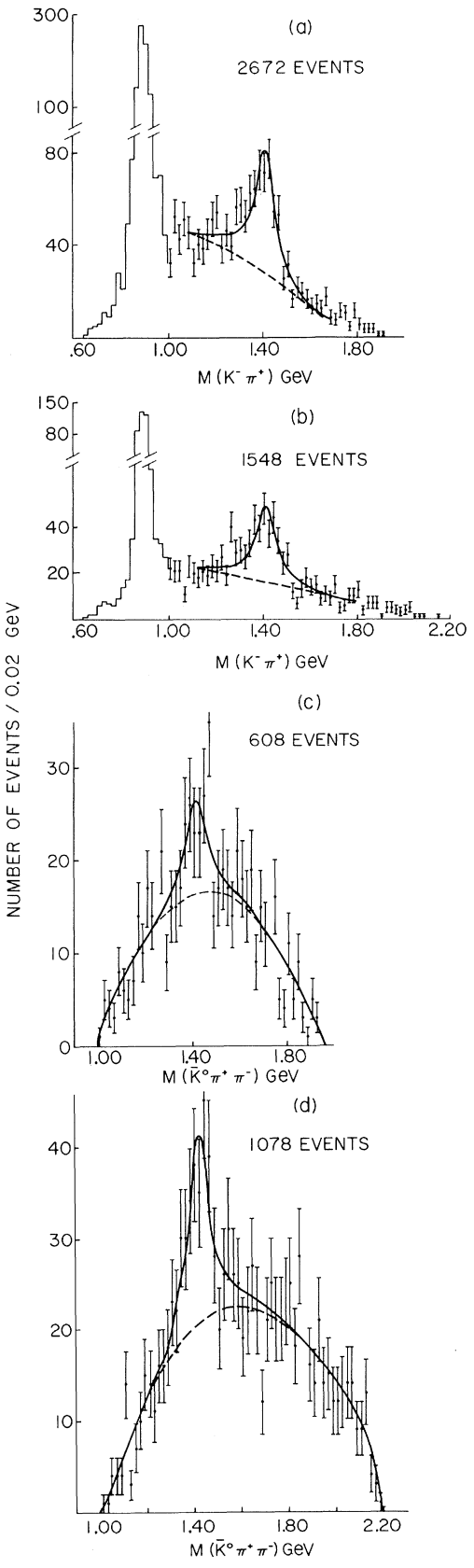


have limited statistics and/or derive this ratio from reactions involving $Q$ production so that they are subject to uncertainties in the determination of the $K\pi\pi$ mode. Our results are of greater statistical validity and are relatively free of systematic errors. The present experiment disagrees with two recent experiments, those of Bishop et al.[11] and Bassompierre et al.,[12] which report a ratio $K(890)\pi/K\pi = 0.93 \pm 0.11$ and $0.9 \pm 0.2$, respectively. These differ from our value by $\sim 4\sigma$ and $\sim 2\sigma$, respectively. In particular, the error quoted by Bishop et al.[11] appears to be unrealistically small. It should also be noted that branching ratios reported here are in excellent agreement with those expected from an unbroken-SU(3) analysis of the $2^+$ nonet,[13] the predicted ratio $K\pi:K(890)\pi:K\rho$ being 50:16:7 for an unsplit $A_2$ and 54:24:6 for a split $A_2$, compared with our experimental ratios of 50:22:7.

Other decay modes were sought by investigating $K(1420)$'s produced recoiling against a proton. These involve Reactions (3)-(6). Because of the predominance of the production of the $Q$ enhancement, Reactions (4) and (5) are ill-suited for the determination of the $K(1420) \to K\pi\pi$ decay mode. This is illustrated in Fig. 3 where the $(K\pi\pi)^-$ effective mass is plotted for 13 816 events of Reaction (4) and 4942 events of Reaction (5) for the combined sample at 3.9 and 4.6 GeV/$c$. It is clearly very difficult to estimate the number of $K(1420)$ events. Even when the peripherally produced events ($\cos\theta^* > 0.9$) are removed, the $K(1420)$ signal-to-noise ratio is only marginally improved (shaded area in Fig. 3). Using the number of $K(1420)$ events obtained from a fit to the $\bar{K}^0\pi^-$ mass spectrum from Reaction (3) (not shown) and the $K\pi/K\pi\pi$ branching fraction derived from Reactions (1) and (2), the number of $K(1420)$ events in the corresponding $K\pi\pi$ spectrum of Reactions (5) and (6) has been estimated. The curve shown in Fig. 3 is the result of a fit which includes this number of $K(1420)$ events. The predicted number of events is consistent with the observed signal, but it is apparent that a branching ratio determination based on this channel would be subject to large uncertainties.

FIG. 2. (a) $K^-\pi^+$ effective-mass spectrum from Reaction (2) at 3.9 GeV/$c$ for events with $\cos\theta^* > 0.08$. (b) Same as (a) but at 4.6 GeV/$c$. (c) $\bar{K}^0\pi^-\pi^+$ effective-mass spectrum from Reaction (1) at 3.9 GeV/$c$ for events with $\cos\theta^* > 0.8$. (d) Same as (c) but at 4.6 GeV/$c$. The curves are the results of the fits described in the text.

Table I. $K(1420)$ decay modes.

| Final state | Selection | Number of observed events 3.9 GeV/$c$ | 4.6 GeV/$c$ | Corrected cross sections[a] ($\mu$b) 3.9 GeV/$c$ | 4.6 GeV/$c$ |
|---|---|---|---|---|---|
| $\overline{K}^0\pi^-\pi^+/n$ | $\cos\theta^*>0.8$ | $70\pm22$ | $149\pm29$ | $46\pm14$[b] | $67\pm13$[b] |
| $K^-\pi^+/n$ | $\cos\theta^*>0.8$ | $333\pm20$ | $242\pm28$ | $125\pm13$ | $173\pm23$ |
| $\overline{K}^0\pi^-/p$ | | $381\pm35$ | | $97\pm9$[b] | |
| $K^-\omega/p$ | | $67\pm50$ | | $8\pm6$[c] | |
| $K^-\eta/p$ | | $0\pm6$ | | $\leq 6$[c,d] | |
| | | Branching ratios | | | |
| $K^*\pi/K\pi$ | $K\rho/K\pi$ | $K\omega/K\pi$ | | $K\eta/K\pi$ | |
| $0.44\pm0.09$ | $0.15\pm0.06$ | $0.05\pm0.04$ | | $\leq 0.04$[d] | |

[a] Corrected for probability cuts.
[b] Corrected for unseen $K^0$ decay.
[c] Corrected for unseen resonance decays.
[d] Two-standard-deviation upper limit.

The $K^-\eta$ and $K^-\omega$ effective mass spectra[14] for Reaction (6) at 3.9 and 4.6 GeV/$c$ were examined (not shown) and the numbers of $K(1420)$ events extracted in the manner indicated above. The corrected cross sections for these two channels are noted in Table I. The $K\eta/K\pi$ and $K\omega/K\pi$ branching ratios derived from these numbers, and given in Table I, are consistent with the world averages and agree with the SU(3) predictions.

We conclude by stating that we have measured the $K(1420)$ branching ratios from a study of reactions in which the $K(1420)$ signal is unambiguous. The $K(890)\pi/K\pi$ ratio differs from the world average and agrees with that predicted by an SU(3) analysis of the $2^+$ nonet.

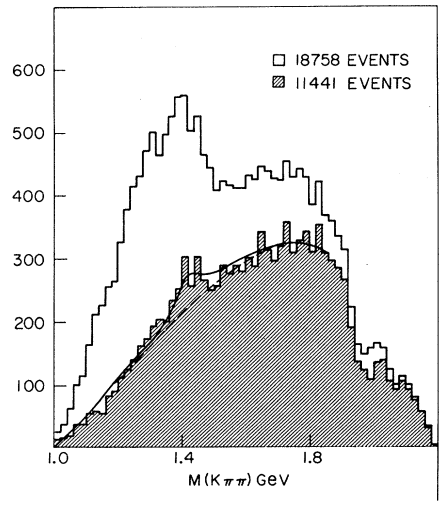


FIG. 3. $(K\pi\pi)^-$ effective-mass spectrum from Reactions (4) and (5). The shaded area is the same mass spectrum but for events with $\cos\theta^*<0.9$. The curve represents the represents the result of a fit in which the number of $K(1420)$ events is fixed at the value predicted from the branching ratio derived in the text, and in which a polynomial background is used.

The support of Dr. R. P. Shutt is gratefully acknowledged as well as the help of Dr. D. Pandoulas. We also thank the alternating-gradient-synchrotron and 80-in. bubble-chamber staffs and crews for their help in obtaining the pictures, and our scanning, measuring, and data handling personnel for their efforts.

---

*Work performed under the auspices of the U. S. Atomic Energy Commission.

[1] B. Maglić, in *Proceedings of the Lund International Conference on Elementary Particles*, edited by G. von Dardel (Berlingska Boktryckeriet, Lund, Sweden, 1970), p. 269.

[2] See references given by A. Barbaro-Galtieri *et al.*, Rev. Mod. Phys. 42, 87 (1970).

[3] The numbers of events per microbarn for topologies 2-prong, 2-prong + $V$, and 4-prong are 2.7, 5.1, and 6.4 at 3.9 GeV/$c$ and 1.4, 7.4, and 3.6 at 4.6 GeV/$c$, respectively. At 5.0 GeV/$c$ only the 2-prong + $V$ events were measured (2.1 events/$\mu$b); these data have been used only for the Dalitz plot analysis. The quoted numbers include scanning and measuring efficiencies.

[4] The expression used in the $\chi^2$ fit to the mass spectrum is $dN/dm = A(1+\epsilon f_{BW})$, where $A$ is a polynomial of the form

$$A=\sum_{l=0}^{n} a_l m^l$$

and $f_{BW}$ is a Breit-Wigner shape with parameters $M$ = 1423 MeV and $\Gamma$ = 101 MeV as determined by P. J. Davis *et al.*, Phys. Rev. Lett. 23, 1071 (1969). The order of the polynomial used corresponds to that giving the best $\chi^2$ probability, and is never greater than five. The same technique has been used to extract the number of resonance events throughout the paper. The

backgrounds obtained in this manner are indicated as the dashed curves in the figures.

[5]Interferences between resonance and background have been neglected as well as interferences between the decay modes of the $K(1420)$. A good fit to the Dalitz plot has been obtained without invoking interference effects, whose inclusion greatly increases the number of parameters.

[6]Instead of the simple $|f_{BW}|^2 \sin^2\theta$ density function we have also used $[(\vec{p}\times\vec{q})^i \cdot \vec{p}^j + (\vec{p}\times\vec{q})^j \cdot \vec{p}^i]^2 |f_{BW}|^2 \sim p^4 q^2 \sin^2\theta |f_{BW}|^2$, which takes into account angular-momentum barriers, where $\vec{p}$ is the momentum of the vector meson in the $K(1420)$ rest frame and $\vec{q}$ is the momentum of one of the decay particles in the $1^-$ rest frame. The branching ratios so obtained agree within one-half standard deviations with the ones quoted in the text. We have used

$$|f_{BW}|^2 = \frac{m}{q}\,\frac{\Gamma}{(m^2-m_0^2)^2+m_0^2\Gamma^2}$$

with $\Gamma=\Gamma_0(q/q_0)^{2l+1}$, $m_0=0.895$ (0.760) GeV, and $\Gamma_0=0.050$ (0.130) GeV for the $K(890)$ ($\rho$).

[7]We assume that only quasi two-body decay modes of the $K(1420)$ are present. The fit has also been performed allowing an uncorrelated $K\pi\pi$ decay mode without any significant improvement in the likelihood function.

[8]An estimation of the parameters $\beta_1$ and $\beta_2$ has been obtained by fitting the Dalitz plots in 160-MeV bands a adjacent to the $K(1420)$ and linearly interpolating the $K(890)\pi$ and $K\rho$ ratios into the $K(1420)$ region. The values used for the Dalitz plot analysis are $\beta_1=0.57$ and $\beta_2=0.06$.

[9]A $\chi^2$ test on the $K(1420)$ Dalitz plot gives a probability of 10%.

[10]Neglecting decay modes other than the $K\pi$, $K(890)\pi$, and $K\rho$, the decay rates are 0.63, 0.28, and 0.09, respectively.

[11]J. M. Bishop *et al.*, Nucl. Phys. B9, 403 (1969).

[12]G. Bassompierre *et al.*, Nucl. Phys. B13, 198 (1969).

[13]E. Flaminio *et al.*, BNL Report No. 14572 (unpublished).

[14]The resonance bands were defined as $0.535 \leq M(\pi^+\pi^-\pi^0) \leq 0.565$ GeV for the $\eta$ and $0.75 \leq M(\pi^+\pi^-\pi^0) \leq 0.81$ GeV for the $\omega$.

# Polarization of High-Energy Photons Using Highly Oriented Graphite*

C. Berger, G. McClellan, N. Mistry, H. Ogren, B. Sandler, J. Swartz, and P. Walstrom
*Laboratory of Nuclear Studies, Cornell University, Ithaca, New York 14850*

and

R. L. Anderson, D. Gustavson, J. Johnson, I. Overman, R. Talman, B. H. Wiik, and D. Worcester
*Stanford Linear Accelerator Center, Stanford University, Stanford, California 94305*

and

A. Moore
*Union Carbide Corporation, Carbon Products Division, Parma, Ohio 44130*

(Received 26 August 1970)

We have demonstrated the feasibility of a new method of polarizing high-energy photons, by preferential attenuation of photons polarized in one plane as a result of coherent pair production on passage through a single crystal of specific orientation. Highly oriented graphite is a particularly favorable material. The method, feasible at presently available energies, is predicted to be especially useful at higher energies.

In 1962, Cabibbo, Da Prato, De Franceschi, and Mosco[1] suggested a new method for producing linearly polarized $\gamma$-ray beams. Just as visible light can be polarized by being passed through an anisotropic absorber (such as Polaroid film), so also could high-energy photons be polarized. The suggested anisotropic media were copper or silicon single crystals oriented at specific angles to the beam. In this orientation the cross section for coherent electron-pair production from the crystal is different for photons polarized in and normal to the plane of incidence. Since this process contributes substantially to the total cross section at high energy, polarization of the unabsorbed photons results.

At the time this method was suggested, coherent bremsstrahlung from crystals was known to be a feasible source of polarized photon beams. This was due to the theory of Überall[2] and the experiments of Bologna, Diambrini, and Murtas.[3] Subsequent work has further clarified the understanding of this process.[4] For experimental use, polarized-photon beams produced in this way have three important deficiencies. First, the polarization is large only for those photons of energy substantially less than the incident elec-